Luminescence of Ce doped LaCl$_3$ microcrystals incorporated into a single-crystalline NaCl host

Luminescence of Ce doped LaCl₃ microcrystals incorporated into a single-crystalline NaCl host

V V Vistovskyy[1], P V Savchyn[1], G B Stryganyuk[2,3], A S Voloshinovskii[1] and M S Pidzyrailo[1]

[1] Ivan Franko National University of Lviv, 8 Kyryla and Mefodiya Street, 79005 Lviv, Ukraine
[2] HASYLAB at DESY, Notkestraße 85, 22607 Hamburg, Germany
[3] Institute for Materials, SRC 'Carat', 202 Stryjska Street, 79031 Lviv, Ukraine

E-mail: savchynp@gmail.com

Abstract
Formation of LaCl₃:Ce microcrystals embedded in an NaCl host has been revealed for NaCl–LaCl₃ (1 mol%)–CeCl₃ (0.05 mol%) composition by means of scanning electron microscopy (SEM) and luminescence spectroscopy techniques. Scanning electron microscopy has shown the size of LaCl₃:Ce microcrystals to be in the 10–100 μm range. Spectral-kinetic characteristics of NaCl–LaCl₃ (1 mol%)–CeCl₃ (0.05 mol%) luminescence have been studied upon excitation in the ultra violet–visible ultraviolet (UV–VUV) spectral range. Luminescent properties of LaCl₃:Ce microcrystals in NaCl–LaCl₃ (1 mol%)–CeCl₃ (0.05 mol%) are shown to be substantially similar to those of bulk LaCl₃:Ce (1 mol%) crystal. The energy transfer mechanism from the NaCl host and LaCl₃ microcrystal to cerium centres is discussed.

1. Introduction

La-containing LaX₃ and K₂LaX₅ (X = Cl, Br, I) single crystals doped with Ce³⁺ ions have been extensively studied in recent years due to their attractive scintillation characteristics: high scintillation light yield and good energy resolution [1]. The same systems can be model objects for the study of luminescence processes such as up-conversion, down-conversion, cross-relaxation, etc in impurity rare-earth ions [2]. Unfortunately, the bulk crystals of these compounds possess a considerable hygroscopicity. Embedding of La-based microcrystals into halide matrices is considered by us to be one of the promising solutions to this problem. The formation of the Ce³⁺ doped K₂LaCl₅ microphase embedded into a KCl host has already been shown on KCl–LaCl₃–CeCl₃ crystals [3]. The luminescent characteristics of Ce³⁺ doped K₂LaCl₅ microcrystals was found to be comparable with those of bulk K₂LaCl₅:Ce crystals.

Among the crystals mentioned above, LaCl₃:Ce is the most studied crystal in respect of its scintillation properties and luminescence mechanisms [4–7]. In this paper, we report on the luminescent–kinetic properties of NaCl–LaCl₃ (1 mol%)–CeCl₃ (0.05 mol%) crystal. In the case of the NaCl–LaCl₃ (1 mol%) system, the formation of embedded LaCl₃ microcrystals is supposed to occur upon temperature annealing. This follows from the absence of any stable ternary compound in the phase diagram of the NaCl–LaCl₃ solution. Thus, the activating of NaCl with LaCl₃ (1 mol%) and CeCl₃ (0.05 mol%) is expected to result in the formation of cerium doped LaCl₃ microcrystals embedded in the NaCl host.

2. Experiment

A single crystal of NaCl–LaCl₃ (1 mol%)–CeCl₃ (0.05 mol%) composition was grown in a quartz ampoule with previously purified NaCl, LaCl₃ and CeCl₃ using a modified Bridgman–Stockbarger technique. The LaCl₃ (99.9% purity), CeCl₃ (99.5% purity) and NaCl (99.99% purity) raw materials were commercially obtained from Manufacture of Rare Metals Compounds (Russia). The obtained crystal underwent annealing at 600 K for 48 h with the purpose of facilitating the thermal-activated migration of ions and vacancies, resulting in the formation of LaCl₃:Ce microcrystals embedded in the NaCl host. The investigated samples were prepared in a dry atmosphere.

Time-resolved measurements of luminescence excitation and emission spectra as well as the luminescence decay kinetics were performed by excitation using the synchrotron radiation from the DORIS III storage ring (DESY, Hamburg) at the facility of the SUPERLUMI station at HASYLAB [8]. The measurements were carried out at $T = 9$ and 300 K. Emission spectra with a resolution of 5 Å were measured within the 200–650 nm range using an ARC 'Spectra Pro 308' 30 cm monochromator-spectrograph equipped with the CCD detector and HAMAMATSU R6358P photomultiplier tube (PMT). The luminescence excitation spectra were scanned with a resolution of 3.2 Å within 3.7–25 eV by the primary 2 m monochromator in a 15° McPherson mounting using the PMT at the secondary ARC monochromator. Simultaneously with the time-integrated luminescence spectra-integrated component, the time-resolved spectra in two time windows were registered. The fast emission components were selected within the 2–10 ns time-gate and the slow one—within the 100–185 ns gate after the excitation pulse. The repetition period of the excitation pulses was fixed at 198 ns upon operation of the DORIS III storage ring in the five-bunch mode.

3. Results and discussion

3.1. SEM analysis

The microstructure of the NaCl–LaCl$_3$ (1 mol%)–CeCl$_3$ (0.05 mol%) sample is shown in figures 1(a) and (b). Embedded microcrystals of 10–100 μm size are observed on the microphotos. The electron beam analysis has shown the microcrystalline inclusions to contain La and Cl elements in a mass ratio that corresponds to the LaCl$_3$ compound. In the cathodoluminescence mode, these microcrystals are observed as light emitting areas (see figure 1(c)). This fact can be considered as evidence for the preferable incorporation of Ce^{3+} ions into the microcrystals. In the other case, emission of Ce^{3+} would be registered in the cathodoluminescence mode from the entire cleavage face of NaCl–LaCl$_3$ (1 mol%)–CeCl$_3$ (0.05 mol%). The presence of Ce^{3+} ions was not revealed by electron beam analysis due to their small content in LaCl$_3$ microcrystallites.

3.2. Luminescence spectroscopy study

Upon excitation of the NaCl–LaCl$_3$ (1 mol%)–CeCl$_3$ (0.05 mol%) crystal with 4.43 eV quanta ($\lambda_{exc} = 280$ nm), its emission spectra show two luminescent bands peaked at 337 nm (3.67 eV) and 361 nm (3.43 eV) at $T = 9$ K (figure 2(a), curve 1). The luminescence in these maxima shows the dominant fast component (figure 2(a), curves 2) with the excitation maxima in the 4.1–5.5 eV range (figure 3(a), curve 2) characteristic for the interconfigurational 5d $\leftrightarrow$ 4f transitions of Ce^{3+} ions in the LaCl$_3$ host (figure 3(c)). Thus, the spectral-kinetic parameters of 337 and 361 nm emission bands match well with the ones of Ce^{3+} 5d $\rightarrow$ 4f luminescence (335 and 360 nm) from the bulk LaCl$_3$:Ce crystal (figure 2(d), curve 1). Hence, 337 and 361 nm emission bands of NaCl–LaCl$_3$ (1 mol%)–CeCl$_3$ (0.05 mol%) originate from
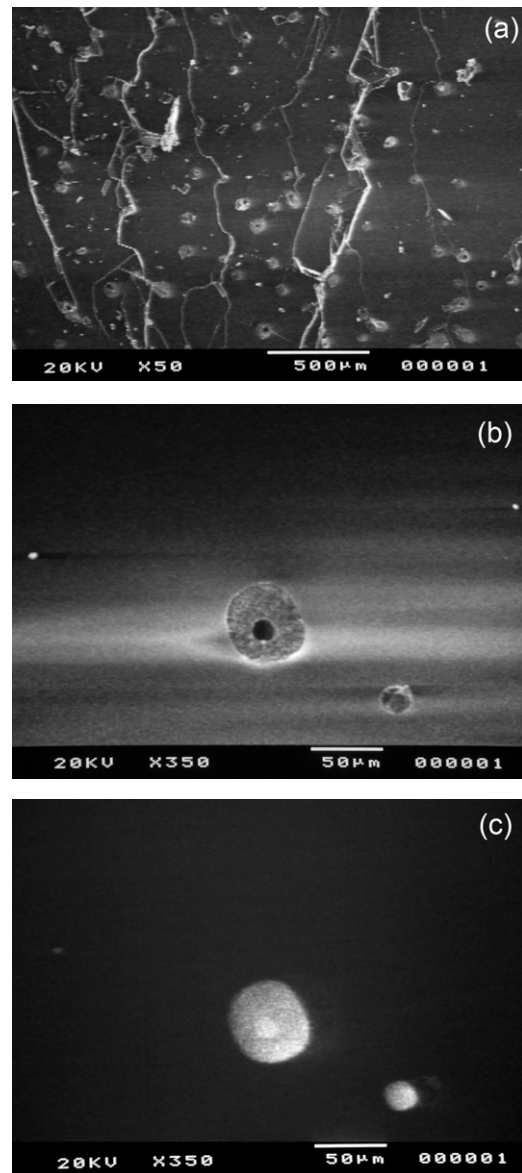

Figure 1. Microphotos of cleaved NaCl–LaCl$_3$ (1 mol%)–CeCl$_3$ (0.05 mol%) obtained by the electron beam analysis technique with different magnification in the secondary electron mode ((a), (b)) and in the cathodoluminescence mode (c).

the radiative relaxation of Ce^{3+} from the excited 5d state to the ^{2}F$_{5/2}$ and ^{2}F$_{7/2}$ terms of the ground 4f state.

From the compositions of the revealed microphase, distribution of the Ce^{3+} impurity and its luminescent characteristics in NaCl–LaCl$_3$ (1 mol%)–CeCl$_3$ (0.05 mol%), we conclude that formation of LaCl$_3$:Ce microcrystals embedded in the NaCl host for the NaCl–LaCl$_3$ (1 mol%)–CeCl$_3$ (0.05 mol%) system has occurred.

Upon excitation of NaCl–LaCl$_3$ (1 mol%)–CeCl$_3$ (0.05 mol%) in the fundamental absorption range of the microcrystalline LaCl$_3$ host ($E_{exc} = 6.88$ eV, $\lambda_{exc} = 180$ nm), beside the doublet of fast Ce^{3+} 5d $\rightarrow$ 4f luminescence (figure 2(b), curve 2), a broad band of slow emission is observed (figure 2(b), curve 3). The spectral position and shape of the slow emission band match the characteristics of typical in-
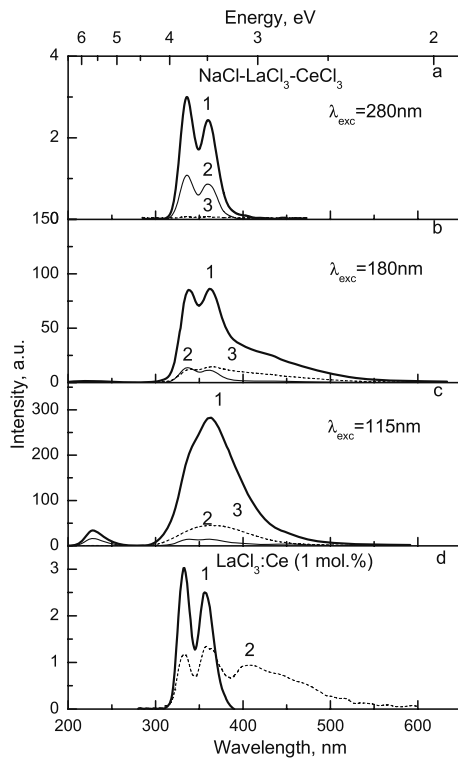
Figure 2. Luminescence spectra of the NaCl–LaCl$_3$ (1 mol%)–CeCl$_3$ (0.05 mol%) crystal (a, b, c: 1—integral, 2—fast, 3—slow components) and LaCl$_3$:Ce (1 mol%) single crystal (d: 1—fast ($\lambda_{exc} = 253$ nm), 2—slow ($\lambda_{exc} = 204$ nm) components).

Figure 3. Excitation spectra of NaCl–LaCl$_3$ (1 mol%)–CeCl$_3$ (0.05 mol%) ((a), (b)) and LaCl$_3$:Ce (1 mol%) single crystals (c), where 1—integral, 2—fast, 3—slow components, 4—reflection spectrum of NaCl–LaCl$_3$ (1 mol%)–CeCl$_3$ (0.05 mol%).
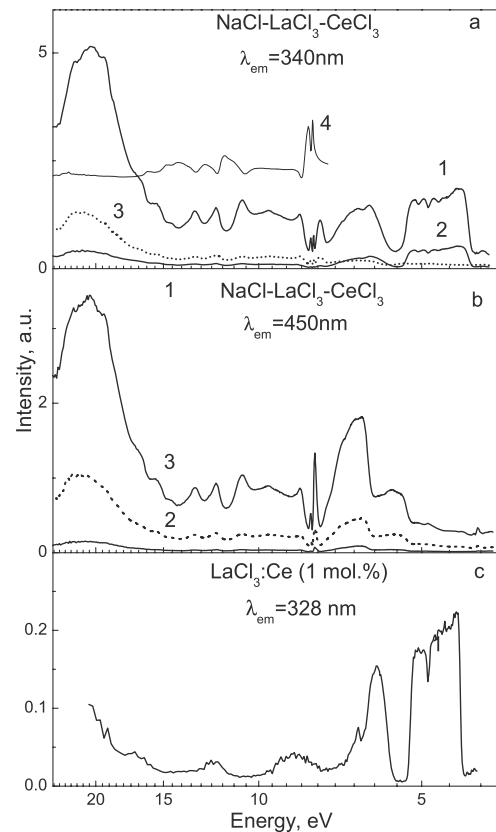
trinsic luminescence of LaCl$_3$ (figure 2(d), curve 2) originating from the radiative recombination of self-trapped excitons (STEs) [7]. The doublet of Ce^{3+} emission is observed in the spectrum of the slow component due to the delayed processes of Ce^{3+} recombinational excitation.

Broad emission bands at 225 nm (5.5 eV) and 364 nm (3.4 eV), originating from the σ- and π-components of STEs in the NaCl host [9] and cerium emission bands are observed (figure 2(c)) in the emission spectrum of NaCl–LaCl$_3$ (1 mol%)–CeCl$_3$ (0.05 mol%) upon excitation with the 10.77 eV quanta ($\lambda_{exc} = 115$ nm) at $T = 9$ K.

3.3. Luminescence excitation spectra

The excitation spectra of Ce^{3+} luminescence in NaCl–LaCl$_3$ (1 mol%)–CeCl$_3$ (0.05 mol%) (figure 3(a), curves 1–3) show the efficiency of Ce^{3+} excitation in the range of (i) the interconfigurational Ce^{3+} 4f $\rightarrow$ 5d absorption (4.1–5.2 eV), (ii) intrinsic absorption of the LaCl$_3$ microcrystalline matrix (5.7–7.4 eV) and (iii) the fundamental absorption range of the NaCl host (7.8–25 eV). The integrated and fast components of Ce^{3+} excitation in NaCl–LaCl$_3$ (1 mol%)–CeCl$_3$ (0.05 mol%) (figure 3(a), curves 1, 2) reproduce roughly the structure of Ce^{3+} 5d $\rightarrow$ 4f transitions in the LaCl$_3$ host [4, 7] (figure 3(c)) within the 4.1–5.2 eV range.

The broad excitation bands of NaCl–LaCl$_3$ (1 mol%)–CeCl$_3$ (0.05 mol%) 450 nm emission within 5.2–7.6 eV corresponds to the intrinsic absorption in the embedded LaCl$_3$

microcrystals. Hence, the excitation of Ce^{3+} emission within 5.7–7.4 eV (figure 3(a), curves 1, 2) corresponds to the energy transfer from the LaCl$_3$ microcrystalline host to the impurity Ce^{3+} ions.

Upon the excitation of NaCl–LaCl$_3$ (1 mol%)–CeCl$_3$ (0.05 mol%) in the range of NaCl fundamental absorption (7.8–25 eV), the doublet of Ce^{3+} emission overlaps the π-component of STE luminescence from the NaCl host (figure 2(c)). Therefore, it is difficult to define concretely the features of Ce^{3+} excitation from the spectrum (figure 3(a)) reproducing the excitation of intrinsic luminescence in a pure NaCl crystal [10] within the 7.8–25 eV range (figure 3(b)). The excitation energy exceeding 16 eV gives rise to the multiplication of electronic excitations in the NaCl host. Therefore, the luminescence excitation spectrum of cerium emission in the range of band-to-band absorption of the NaCl host reproduces the features of the STE luminescence excitation spectrum. It would seem that this feature could be caused by the energy transfer from excitons and electron–hole pairs to microparticles. However, in our previous studies of the luminescence properties of CsPbCl$_3$ nanoparticles embedded in CsCl, RbCl and KCl matrices [11, 12] upon the band-to-band excitation the energy transfer from host matrices to nanoparticles was not observed except for cases of intrinsic or impurity emission reabsorption by nanocrystals. The excitation of nanocrystal luminescence was observed only in the range of
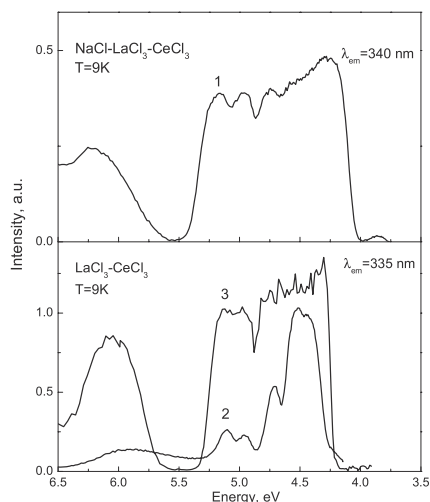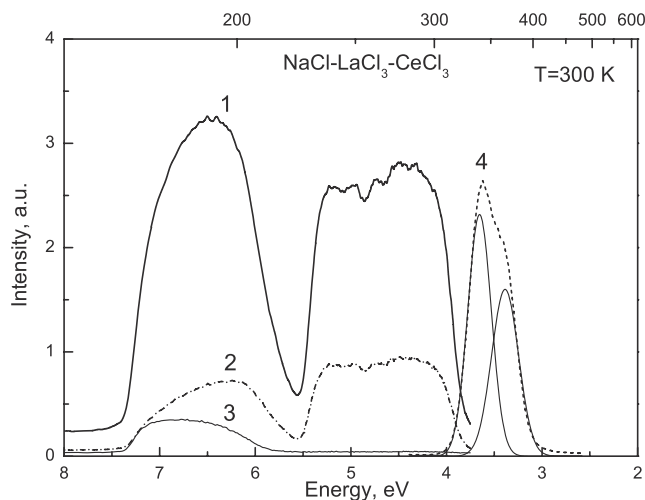
Figure 4. Excitation spectrum of NaCl–LaCl$_3$ (1 mol%)–CeCl$_3$ (0.05 mol%) (curve 1). Excitation spectra of cerium luminescence in the LaCl$_3$:Ce crystal at different activator concentrations (2–0.1 mol%; 3–1.0 mol%).

Figure 5. Excitation (curves: 1—integral, 2—fast, 3—slow components) and luminescence (curve 4) spectra of NaCl–LaCl$_3$ (1 mol%)–CeCl$_3$ (0.05 mol%) crystal at room temperature.

host matrix transparency due to the direct absorption of light by nanocrystals. These facts allow us to suppose that excitation of cerium emission in the range of NaCl host matrix absorption is probably the result of: (i) the overlapping of the π-component of STE emission of NaCl with the cerium luminescence band; (ii) the overlapping of the σ-component of STE emission of NaCl around 220–260 nm with the cerium 4d–5f absorption band.

Correlation between the excitation and reflection spectra is clearly observed for NaCl–LaCl$_3$ (1 mol%)–CeCl$_3$ (0.05 mol%) within the 7.7–16 eV range (figure 3(a), curves 1, 4). The peaks in the reflection spectra coincide with the troughs in the excitation spectra. Such an effect is caused by the nonradiative decay of electronic excitation on the surface defects upon a strong absorption of the excitation quanta within a thin outer layer of the crystal. The nonradiative losses are especially high in the range of a strong excitonic absorption (7.8–8.2 eV) where the penetration depth of the excitation quanta decreases dramatically.

Figure 4 shows the detailed structure of Ce^{3+} excitation in NaCl–LaCl$_3$ (1 mol%)–CeCl$_3$ (0.05 mol%) (frame a, curve 1) and in the LaCl$_3$ bulk host (frame b, curves 3, 4) within the range of the Ce^{3+}4f $\rightarrow$ 5d interconfigurational transition. Regarding the features of the excitation spectrum of NaCl–LaCl$_3$ (1 mol%)–CeCl$_3$ (0.05 mol%) (figure 4, curve 1) and LaCl$_3$:Ce (0.1 mol%) (figure 4, curve 2) in the range of cerium 4f–5d absorption it is clearly visible that in the former the structure of the excitation luminescence band is blurred and its half-width increases, such behaviour is characteristic for a saturated excitation spectrum, which is proper for high impurity concentrations. Because the direct determination of impurity concentration is complicated, we can only try to estimate roughly the concentration of impurity Ce^{3+} ions for LaCl$_3$ microcrystallites in NaCl–LaCl$_3$ (1 mol%)–CeCl$_3$ (0.05 mol%) from the form of the cerium excitation band. On the basis of concentrations of LaCl$_3$ and CeCl$_3$ components

in the melt, the upper limit of cerium concentration in microcrystals may be evaluated to be around 5 mol% under the assumption that whole cerium has entered the microphase. Comparing the structure of Ce^{3+}4f $\rightarrow$ 5d excitation spectra for LaCl$_3$:Ce (0.1 mol%), LaCl$_3$:Ce (1 mol%) and NaCl–LaCl$_3$ (1 mol%)–CeCl$_3$ (0.05 mol%) we can assume that the concentration of cerium in microcrystals is more than 0.1 mol%.

3.4. Excitation at room temperature

Emission of impurity Ce^{3+} ions is observed at 339 nm (3.65 eV) and 365 nm (3.39 eV) upon the excitation of NaCl–LaCl$_3$ (1 mol%)–CeCl$_3$ (0.05 mol%) within the absorption range of embedded LaCl$_3$ microcrystallites at room temperature (figure 5, curve 4). The intrinsic luminescence of the LaCl$_3$ microcrystals is not detected at room temperature. The excitation spectrum of Ce^{3+} luminescence shows the broadening of Ce^{3+}4f $\rightarrow$ 5d absorption bands. The low-energy edge of Ce^{3+}4f $\rightarrow$ 5d absorption is shifted into the long-energy range at room temperature versus low temperature. Ce emission at excitation in this band has only a fast decay time component.

The fast and slow components are resolved for the luminescence of Ce^{3+} upon the excitation within the broad band (5.6–7.3 eV) corresponding to the intrinsic absorption of LaCl$_3$ microcrystals (figure 5, curves 2, 3). The fast component prevails at the low-energy side around 6 eV and may be attributed to the excitation of Ce^{3+} due to the energy transfer from the near-activator exciton as it was reported [7] for the bulk LaCl$_3$–Ce (1 mol%) crystal.

3.5. Decay kinetics

Upon excitation of the NaCl–LaCl$_3$ (1 mol%)–CeCl$_3$ (0.05 mol%) crystal with 4.9 eV quanta, the decay kinetics of Ce^{3+} luminescence reveals a single-exponential profile with a decay time constant of 15.9 ± 0.2 ns (figure 6,
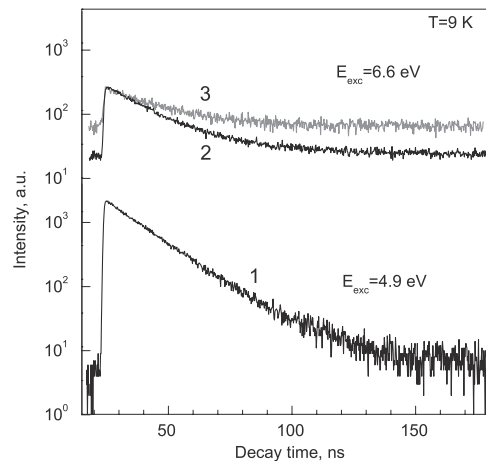
Figure 6. Decay kinetics of cerium luminescence from NaCl–LaCl$_3$ (1 mol%)–CeCl$_3$ (0.05 mol%) (curves 1, 2) and the LaCl$_3$:Ce (1 mol%) single crystal (curve 3).

curve 1). This value of the decay time constant is close to the case of LaCl$_3$:Ce bulk crystal. Both the bulk LaCl$_3$:Ce and NaCl–LaCl$_3$ (1 mol%)–CeCl$_3$ (0.05 mol%) show the pronounced recombinational decay kinetics of Ce^{3+} luminescence (figure 6, curves 2, 3) upon the excitation within the range of electron–hole pair formation in LaCl$_3$ ($E = 6.6$ eV, 180 nm). Two-exponential decomposition of the decay kinetics of Ce^{3+} luminescence from NaCl–LaCl$_3$ (1 mol%)–CeCl$_3$ (0.05 mol%) excited at 6.6 eV gives us the decay time and contribution of the fast 17.7 ± 0.2 ns (26% contribution) and slow 473 ± 50 ns (74% contribution) components. NaCl–LaCl$_3$ (1 mol%)–CeCl$_3$ (0.05 mol%) shows a reduced contribution of the slow component to the decay kinetics of Ce^{3+}5d $\rightarrow$ 4f luminescence as compared with the LaCl$_3$:Ce (1 mol%) bulk crystal. Such changes in the luminescence decay kinetics can be caused by opposing reasons: on the one hand by the decrease of the amount of deep traps responsible for the slow decay component in microparticles but on the other hand by the appearance of new defects at the microphase/NaCl interface leading to nonradiative decay of electron excitation. The energy transfer from LaCl$_3$ to NaCl host can be responsible for such luminescence decay changes, too. The elucidation of the observed luminescence decay behaviour in microcrystals requires additional study.

4. Conclusions

Formation of LaCl$_3$:Ce microcrystals embedded in an NaCl matrix for NaCl–LaCl$_3$ (1 mol%)–CeCl$_3$ (0.05 mol%) crystal after its annealing has been revealed by SEM and luminescence spectroscopy techniques. The characteristics of Ce^{3+}

luminescence of bulk and embedded LaCl$_3$:Ce^{3+} microcrystals are similar.

The cerium emission in NaCl–LaCl$_3$ (1 mol%)–CeCl$_3$ (0.05 mol%) is excited via 4f–5d absorption, energy transfer from the LaCl$_3$ lattice as well as the reabsorption of NaCl host emission. The contribution of the slow component into the decay kinetics of Ce^{3+}5d $\rightarrow$ 4f luminescence in NaCl–LaCl$_3$ (1 mol%)–CeCl$_3$ (0.05 mol%) is shown to decrease, which indicates the defect structure transformation of LaCl$_3$:Ce microcrystals in the NaCl host as compared with LaCl$_3$:Ce (1 mol%) bulk crystal.

The demonstration of the Ce doped LaCl$_3$ microphase creation in the NaCl host opens up the possibility of searching for similar inclusions in other matrices, which is promising for the development of new luminescence materials.

References

[1] Guillot-Noell O, de Haas J T M, Dorenbos P, van Eijk C W E, Kramer K and Gudel H U 1999 *J. Lumin.* **85** 21
[2] Legendziewicz J, Cybińska J, Boulon G and Meyer G 2007 *Opt. Mater.* **29** 1217
[3] Voloshinovskii A, Stryganyuk G, Zimmerer G, Rodnyi P, Antonyak O, Myagkota S and Savchyn P 2005 *Phys. Status Solidi* a **202** R101
[4] Andriessen J, Antonyak O T, Dorenbos P, Rodnyi P A, Stryganyuk G B, van Eijk C W E and Voloshinovskii A S 2000 *Opt. Commun.* **178** 355
[5] Bernabei R, Belli P, Montecchia F, Nozzoli F, d'Angelo A, Cappella F, Incicchitti A, Prosperi D, Castellano S, Cerulli R, Dai C J and Tretyak V I 2005 *Nucl. Instrum. Methods Phys. Res.* A **555** 270
[6] Allier C P, van Loef E V D, Dorenbos P, Hollander R W, van Eijk C W E, Krämer K W and Güdel H U 2002 *Nucl. Instrum. Methods Phys. Res.* A **485** 547
[7] Voloshynovskii A S, Antonyak O T, Stryganyuk G B, Dorenbos P, van Eijk C W E and Rodnyi P A 2002 *Ukr. J. Phys. Opt.* **3** 194
[8] Zimmerer G 2007 *Radiat. Meas.* **42** 859
[9] Song K S and Williams R T 1996 *Self-Trapped Excitons* (Berlin: Springer)
[10] Beaumont J H, Bourdillon A J and Kabler M N 1976 *J. Phys. C: Solid State Phys.* **9** 2961
[11] Myagkota S, Stryganyuk G, Voloshinovskii A, Rodnyi P, Kirm M and Zimmerer G 2004 *Opt. Commun.* **229** 271
[12] Voloshinovskii A, Myagkota S, Gloskovskii A and Zazubovich S 2001 *Phys. Status Solidi* b **225** 257